Soils and Rocks
An International Journal of Geotechnical and Geoenvironmental Engineering
www.soilsandrocks.com
ISSN 1980-9743
ISSN-e 2675-5475

Hydro-geomorphological conditions for the classification of terrain susceptibility to shallow translational landslides: a geo-hydro ecological approach

Roberta Pereira da Silva[1#], Ana Luiza Coelho Netto[2], Willy Alvarenga Lacerda[3]

Article

Keywords
Shallow landslide
Terrain susceptibility
Geomorphological parameters
Geo-hydroecological approach

Abstract

This work is part of the review of methodological procedures for the analysis and classification of terrain susceptibility to shallow translational landslides, following the geo-hydro ecological approach. The pilot area is located in Nova Friburgo (RJ), specifically in the D'Antas Creek basin (53 km^2). At this stage of the work, geomorphological parameters and indices were evaluated, including slope angle, curvature, drainage efficiency index (*DEI*) and topography position index (*TPI*), seen as relevant in regulating the hydrological and mechanical behavior of soils. The results obtained were intersected with an inventory of landslide scars (n = 382) referring to the extreme rainfall event in January 2011, which occurred in the highland region, called Região Serrana, of the state of Rio de Janeiro. This intersection allowed an evaluation between these parameters and the slopes rupture. The concentration of landslide area per class subsidized the establishment of weights for each of the adopted classes, based on the AHP method. A readjustment of the slope angle classes was proposed, as well as the inclusion of the standard curvature in the construction of the Hydro-Geomorphological Conditions Map. The results were promising, with a concentration of 88.74% (0.85 km^2) of the landslide areas in the class of high erosive potential.

1. Introduction

Several methodologies have been described in the literature for classifying landslides susceptibility, including probabilistic analyzes based on long inventories of cases (Casagli et al., 2004; Fell et al., 2008; Martha et al., 2014) and diagnoses based on the crossing of thematic maps (Coelho Netto et al., 2007; Akgun et al., 2008; Bortoloti et al., 2015; Abedini & Tulabi, 2018). The latter still prevails in Brazil, whose information has emphasized the role of the geological and/or geological-geotechnical categories. The inclusion of geomorphological parameters is usually limited to the adoption of slope angle as the main, and sometimes only parameter in terrain susceptibility assessments (Fernandes et al., 2001; Dias et al., 2021a), through a linear vision of its interference in the occurrence of this phenomenon.

Although landslide terrain susceptibility maps are increasingly used, in the way they are presented today, they still have limitations, mainly due to the scale of elaboration and availability of data in adequate quantity and quality. Identifying the factors that control the distribution and occurrence of landslides and determining their relative importance is complex. These phenomena can be triggered under multiple meteorological, geological, geomorphological, vegetation cover, and land use conditions (Guzzetti et al., 2008; Coelho Netto et al., 2013; Borgomeo et al., 2014). The relationship between landslide and triggering factors varies spatially and temporally. Furthermore, the circumstances under which one factor may dominate the others are difficult to assess.

The methodological procedures and the models for evaluating terrain susceptibility to landslides must be dynamic and need to be open to updates at time intervals compatible with the rate and variability of landscape transformations. For this reason, the geo-hydro ecological approach has been adopted for structuring the thematic bases, as well as in the integrated analysis of terrain susceptibility. This approach is based on empirical-analytical and integrative knowledge of indicators and categories relevant to the phenomenon in focus, as summarized in Coelho Netto et al. (2020).

[#]Corresponding author. E-mail address: pereira.roberta00@gmail.com
[1]Universidade Federal do Rio de Janeiro, Programa de Pós-graduação em Engenharia Civil, Rio de Janeiro, RJ, Brasil.
[2]Universidade Federal do Rio de Janeiro, Departamento de Geografia, Rio de Janeiro, RJ, Brasil.
[3]Universidade Federal do Rio de Janeiro, Departamento de Geotecnia, Rio de Janeiro, RJ, Brasil.

Submitted on May 15, 2023; Final Acceptance on October 25, 2023; Discussion open until February 28, 2024.

https://doi.org/10.28927/SR.2023.005623

The integrated analysis aimed at classifying terrain susceptibility involves geological-geotechnical, hydrogeomorphological, vegetation cover, and land use indicators. The systemic view of geographic space, based on multiple (spatial and temporal) scales of analysis, is essential for the geo-hydroecological approach (Coelho Netto et al., 2020).

In one of the methodological review and update stages for classifying terrain susceptibility to shallow landslides, in a detailed scale (between 1:5,000 and 1:10,000), the study by Silva et al. (2022) evaluated the relevant geotechnical parameters in the definition of geological-geotechnical units in the D'Antas Creek basin (53 km^2), in Nova Friburgo (RJ), Brazil. The method proposed by the authors was based on the integration of parameters and indices, such as granulometry, Atterberg limits (*LL, PL, PI, A*), aggregate stability index, void ratio, saturated hydraulic conductivity, *c'* (effective cohesion) *φ'* (internal effective friction angle) for the categorization of terrain units according to the mechanical and hydraulic behavior of the materials. This study enabled the regrouping of the six lithological units, defined by Avelar et al. (2016), in three geological-geotechnical units, based on a functional reading of the geotechnical behavior of soils.

The present work constitutes one more stage of revision of the methodology developed by GEOHECO-UFRJ/ Geo-Hydro Ecology and Risk Management Laboratory (COPPETEC/SMAC-RJ, 2000; Coelho Netto et al., 2007; COPPETEC/SEA -RJ, 2010 and Coutinho, 2015). Now, the focus lies on the functional categorization and improvement of hydro-geomorphological indicators related to the detonation of shallow landslides. An improvement of the tools available in the Geographic Information System (GIS) used in this study was sought, to obtain parameters, such as slope angle and curvature, which were more adequate to the analysis.

2. Materials and methods

To define the hydro-geomorphological conditions, the parameters, and indices were integrated and weighted on a functional basis. The latest reviews of these terrain conditions, prepared by Coutinho (2015) and Coelho Netto et al. (2014), considered a synthesis of the parameters related to the variable set of slopes angles within the landslide scars, however, not discriminating the mean slope angle of each scar. The topography position index (*TPI*) and the drainage efficiency index (*DEI*) were not changed. The curvature of the slopes was not considered. In the early work by Coelho Netto et al. (2007), the hydro-geomorphological map corresponds to the integration of the *DEI* with other functional parameters, including critical slope angles and curvature, combined in the following classes: concave/0–10°, convex-straight/0–10°, concave/10–20°; convex–straight/10–20°; concave/20–35°; convex–straight/20–35°; concave/>35°; convex–straight/>35°.

From these three works, in this research the incorporation of the curvature parameter as another terrain condition was proposed. Despite the recognized importance of curvature (plan and profile) and the gradual insertion of this parameter in models of susceptibility zoning, the curvature remains underestimated as a geomorphological parameter (Catani et al., 2005; Kayastha et al., 2013; Meirelles et al., 2018). The present study was developed in the same study area used by Coutinho (2015), which allowed the use of some formerly produced data, applying the necessary adjustments to adapt to the current proposal.

2.1 Study area

The D'Antas Creek basin (53 km^2) located in Nova Friburgo, a municipality in the highland region of the state of Rio de Janeiro (Figure 1), was defined as a pilot area given the occurrence of hundreds of landslides and the high losses and damages of a social, economic and environmental nature in the last catastrophic event in January 2011. Coelho Netto et al. (2013) identified 3,622 landslide scars, in an area of 421 km^2 (Figure 1b), largely inserted in the municipality of Nova Friburgo and including small areas of Teresópolis and Sumidouro municipalities, out of which more than 80% were concentrated in Nova Friburgo.

Since 2012, GEOHECO-UFRJ has been developing research on the conditions of shallow translational landslides, prevalent in the region. It is a 5th order basin (Strahler, 1952), with altitude varying between 840 m and 2,054 m, according to the Hipsometric model (Coutinho, 2015). The D'Antas Creek is a tributary of the Bengalas River, which drains to the Grande River, a tributary of the Dois Irmãos River. The latter runs into the right bank of the Paraíba do Sul River (regional collector).

High-altitude tropical climate predominates in the Região Serrana, with an annual average temperature of 16ºC, varying between 37º and -2ºC (Coelho Netto et al., 2013). The region's climate is influenced by the Atlantic Tropical air mass, which causes high rainfall, especially in summer. Nova Friburgo is pointed as one of the cities with the highest rainfall rates in the state, with average annual precipitation (1977–2000) around 2500 mm in the highest areas, decreasing progressively in the northern area down to 1,300 mm (Coelho Netto et al., 2008).

The region's characteristic biome is Atlantic Forest, currently fragmented and highly degraded. According to Ribeiro et al. (2009), more than 80% of the forest fragments have less than 50 ha and are more than 1 km apart. The authors claim that these forest remnants occupy from 11.4% to 16% of this region. The vegetation originally present in the study area is included in the phytogeographic classification of Montana Dense Ombrophilous Forest which, according to Veloso et al. (1991), covers the mountains and plateaus between 500 m and 1,500 m high.

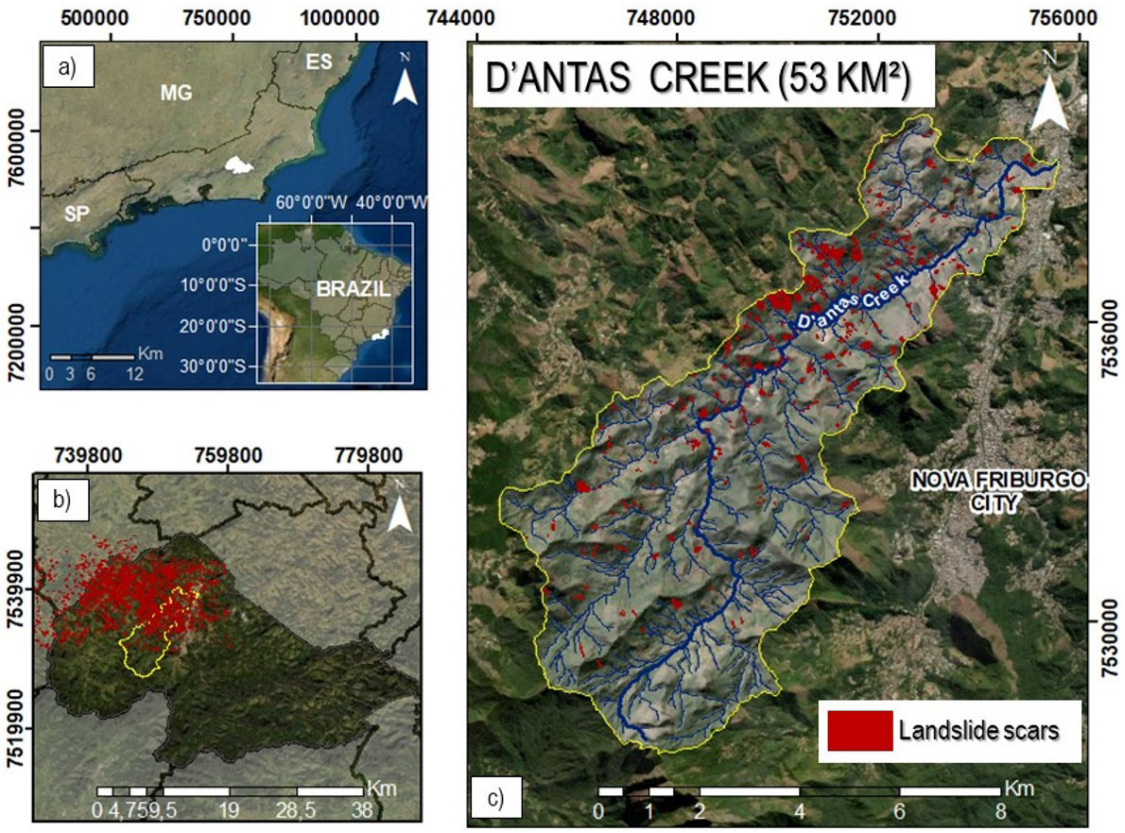

Figure 1. Location map of the D'Antas Creek basin. a) Location of the municipality of Nova Friburgo; b) Location of the D'Antas Creek basin in the context of the municipality. In red, there are the landslide scars mapped in an area of 421 km² by Coelho Netto et al. (2013); c) D'Antas Creek basin and the indication of landslide scars used in the present study.

With the opening and paving of the highway RJ-130, which connects Nova Friburgo to Teresópolis, in the 1970s, a process of transition from rural to urban in the basin area began. The region came to be considered an area of industrial expansion, a fact that accelerated population growth. Currently, the basin comprises eight neighborhoods (D'Antas Creek, Alto Floresta, Dois Esquilos, Ponte Preta, Cardinot, Solaris, Venda das Pedras and Jardim California), with a population of approximately 23,000 people (11% of the population of the municipality) (Coutinho, 2015).

2.2 Landslide Inventory

Based on the landslide inventory from the January 2011 extreme rainfall event prepared by Silva et al. (2016), there was a new visual interpretation of the scars. Using a Geoeye satellite image of high spatial resolution (0.5 m) obtained shortly after the event (May/2011), the contour lines at a scale of 1:5,000 and images provided by *Google Earth Pro* (dated 01/19/2011 and 06/05/2011), the scars were reclassified with a focus on shallow translational landslides and a prioritization of detonation and transport zones.

The landslides previously classified as complex (a combination of two or more types of movements), according to the definition by Varnes (1978), were dismembered to highlight the surfaces of ruptures or erosion zone (Figure 2a). Scars with an elongated shape and incised in the axes of concavities were classified as debris flow at their origin (Figure 2b) and were excluded from this analysis. Scars related to shapes with a wider base were associated with shallow translational slips (Figure 2c).

Considering these new criteria for mapping shallow translational landslide scars, 382 scars with areas between 50 m² and 60,000 m² were counted, totaling around 958,220 m² (0.96 km²) of the landslide area. Despite the great variability in sizes between the mapped polygons, approximately 73% (280) of the scars had an area of up to 2,000 m² and 51% (197) an area of up to 1,000 m².

Based on the distribution of scars, the landslide potential of each class was defined, as observed in the works by Gao (1993), Larsen & Torres-Sánchez (1998), Catani et al. (2005), Nakileza & Nedala (2020), among others. The landslide inventory was used to validate the hydro-geomorphological conditions map, a process through which one sought to define the reliability, robustness, degree of adjustment, and forecasting ability of the proposed model.

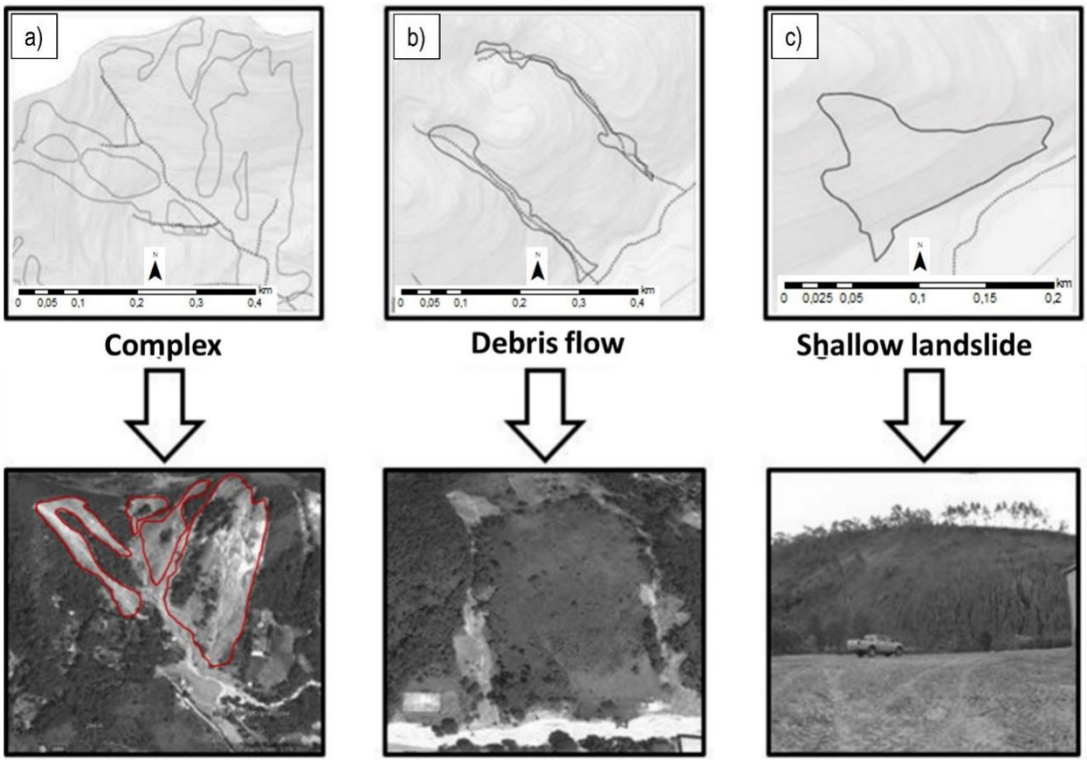

Figure 2. Types of gravitational mass movements considered in the scar inventory produced by Silva et al. (2016); a) Complex movement, which was dismembered from erosion and transport zones by the present study, as indicated by the red polygons; b) Debris flows associated with relief concave compartments, disregarded by this analysis; c) Shallow translational landslide, type of mass movement in focus (Adapted from Silva et al., 2016).

2.3 Hydro-geomorphological conditions

2.3.1 Drainage Efficiency Index (*DEI*)

Data referring to the Drainage Efficiency Index (*DEI*) used in this research were produced by Coutinho (2015). The channel network was traced with the support of the *ArcHydro* tool (ArcGis 10.2) and through field observations, especially in the low hierarchical order sub-basins (up to 2nd order). The higher hierarchical order basins, as well as the lateral slopes that drain directly into the main river channels, were adjusted to the adjacency pattern with the closest neighbors that went through the classification process (Coutinho, 2015). Initially, this author classified the numerical products of the *DEI* as "natural breaks[1]" into four classes (very high, high, medium, and low). However, in the present study, the option was the use of three *DEI* classes: high, medium and low, as proposed by Coelho Netto et al. (2007).

Higher values of *DEI* tend to favor the rainwater flow of surface and subsurface, which converges to the topographic concavity axis, channeled or not (Coelho Netto et al., 2007). The increase in drainage efficiency tends to favor the incision of erosive channels whose incision and regressive growth can destabilize the steep slope and trigger landslides (positive feedback). Like the drainage density parameter, this index translates the time or response capacity of the basin which, together with the topographic gradient of the contribution basin, configures the drainage efficiency, as seen in Equation 1 proposal by Coelho Netto et al. (2007), where:

$$DEI = HDd \times G = \frac{\sum_1^n L_h + \sum_1^n L_c}{A_b} \times \frac{\Delta Z}{L} \quad (1)$$

where: *HDd* is the Hollow-Drainage density, *G* is the basin gradient (non-dimensional), L_h is the total length of hollow axis, L_c is the total length of channels, ΔZ is the basin elevation, L is the basin length and A_b is the basin area.

2.3.2 Slope angle

The slope angle values were extracted from the Digital Terrain Model (DTM) (1:5,000), using the *Slope* tool

[1]The "natural breaks" method adjusts the limits of the classes according to the distribution of the data, identifying breakpoints between the classes from a statistical analysis based on the variability of the data, aiming to minimize the sum of the variance within each of the classes (Jenks, 1977).

(ArcGis 10.7). The generated file was reclassified using the *Reclassify* tool within the same software. The works by Gao (1993), D'Amato Avanzi et al. (2004), Coelho Netto et al. (2007, 2014), Cevasco et al. (2013), Coutinho (2015) were used as a base for the definition of these classes. They discuss the role of slope angle in the detonation of shallow landslides and helped define the following class intervals:

i) 0° to 10°: considered as a potential area for deposition;
ii) 10° to 20°: low potential for landslides, considered an area of use permitted by law;
iii) 20° to 30°: medium landslide potential; area with legal restrictions for human use;
iv) 30º to 45º: critical angles of slope stability rupture, that is, with high potential for landslides;
v) > 45º: unstable slopes, generally with thin soil or rocky cliffs.

The files were converted from raster to vector (polygon) format, using the *Raster to polygon* tool. To define the intervals that best fit the critical angles of the basin, the DTM was extracted from the landslide scar polygons of January 2011 using the *Extract by mask* tool. To this file, containing elevation information only within the polygons of scars, the *Slope* tool was applied. The generated file was reclassified (*Reclassify*) one by one grade (through the manual classification method) covering all slope angles recorded inside the scars, which in this case was from 0° to 69°.

The landslide scars were evaluated individually concerning the mean, maximum, minimum, standard deviation, and frequency of distribution of slope values per scar. Mean slope angle values were assumed to be representative of the polygons. Figure 3 shows an example of how the reading of slope angle values was performed in each scar.

2.3.3 Curvature

The curvature of the slopes was also obtained from the DTM, using the *Curvature* tool (ArcGis 10.7). It was decided to work with the standard curvature, due to the greater possibility of understanding the role played by the concave portions of the relief in the convergence of superficial and shallow subsurface flows and consequent instability of the slopes.

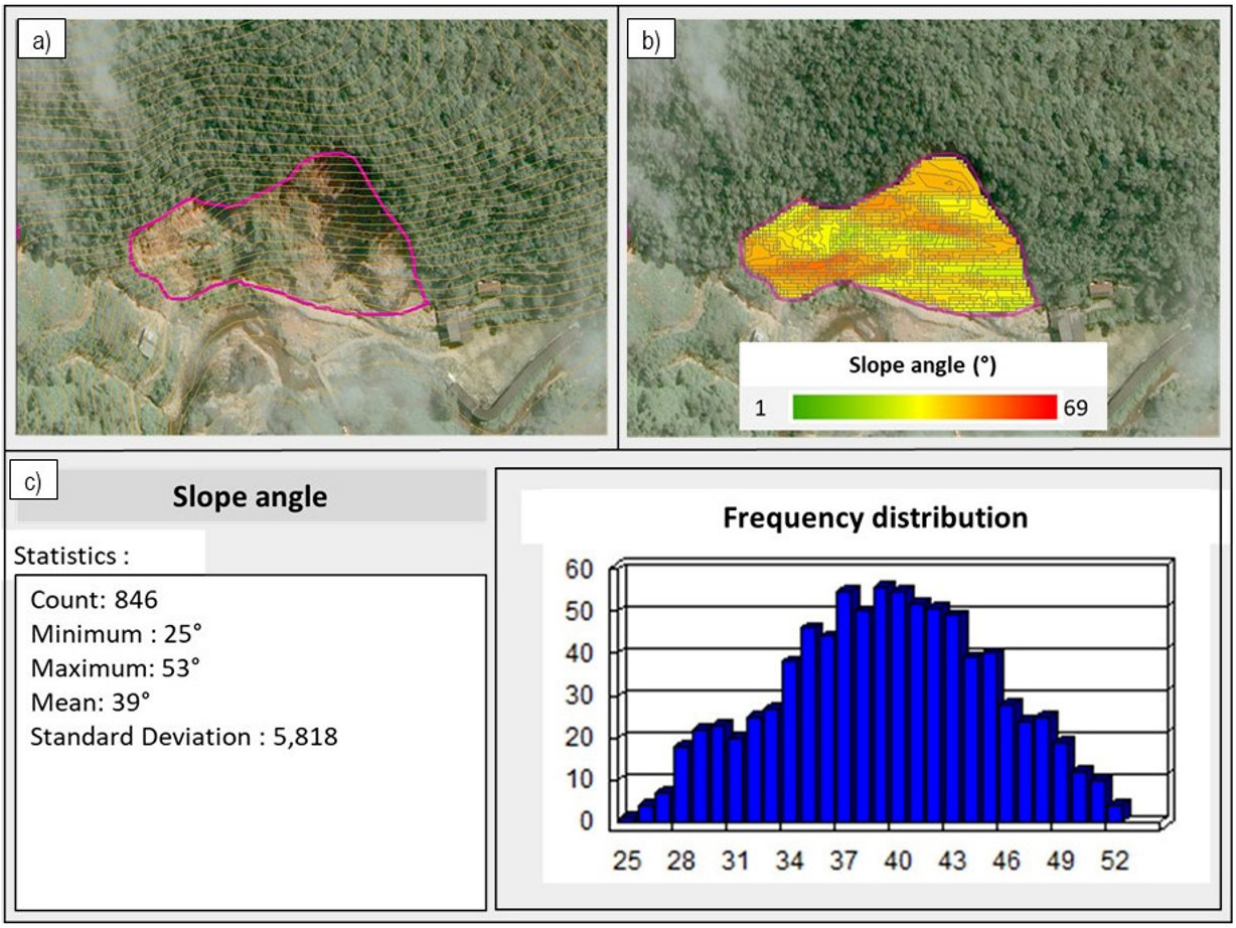

Figure 3. Morphological and topographical analysis of slipping scars. a) Example of scar demarcation with contour line (1:5,000); b) Example of data analysis referring to the distribution of slope angle values along the scar; c) Adapted model of how data is processed and presented by the software used (ArcGis 10.7).

Different intervals were tested in search of the best adjustment of this parameter to the reality of the study area. Initially, the tests were based on the values predefined in the literature (Valeriano, 2008; Tagil & Jenness, 2008; Bortoloti et al., 2015; Wang et al., 2015; ESRI, 2019; Dias et al., 2021b; Nohani et al., 2019), however, none of them proved to be adjusted to the study area.

In general, it was observed that the automated data were overestimating the convex-divergent areas and underestimating the rectilinear-planar areas. This problem was also pointed out by Valeriano (2008). According to the author, there is a need to admit a margin of values greater than zero so that planar slopes can be highlighted. Among the ranges tested, those that best fit the conditions of the D'Antas Creek basin were: values < -0.1 associated with concave-convergent slopes, values between -0.1 and 3.5 related to rectilinear -planar slopes, and values > 3.5 assumed as representative of convex-divergent slopes. These data were extracted from the DTM prior to the occurrence of the landslides. When necessary, supervised revisions were performed to better fit the model to the terrain conditions.

The judgment of the suitability of intervals was based on the mapping of landslide scars about the type of slope curvature, based on visual interpretation. With the aid of a *Geoeye* satellite image with a high spatial resolution (0.5 m), contour lines on a scale of 1:5,000, and a visualization scale between 1:5,000 and 1:3,000, this mapping proved to be essential to define the intervals of curvature. However, it is necessary to highlight that threshold adjustments need to be made depending on local conditions, mapping scale, and type of input data.

2.3.4 Topography Position Index (*TPI*)

The *TPI* has been used to determine the terrain susceptibility to landslide, as presented by Tagil & Jenness (2008), Seif (2014), and Nseka et al. (2019), among others. According to Weiss (2000), many physical and biological processes that act on the landscape are highly correlated with the topographic position. The *TPI* becomes relevant for the analysis of slope stability, as it helps to identify the preferential zones for the occurrence of landslides through the automation of relief classification (Tagil & Jenness, 2008; Seif, 2014).

The data referring to the *TPI* used in this research were produced by Coutinho (2015), based on the criterion defined by Weiss (2000) and the tool proposed by Jenness (2006). These data were generated at a scale of 1:5,000, with a spatial resolution of 2.5 m and radii of 12.5 m, 25 m, 50 m, and 100 m, as presented by Coutinho (2015). Adjustments related to the radii need to be made based on the local conditions of the study area and the scale of analysis. The results were classified using the "*Natural breaks*" method into five classes: i) Ridge; ii) Upper slope; iii) Middle slope; iv) Lower slope; v) Valley bottom (Coutinho, 2015).

2.3.5 Hydro-geomorphological map

Assuming that the forms mirror the processes that gave rise to them, in understanding the geomorphological evolution of the landscape, as advocated by Gilbert (1877), the hydro-geomorphological conditions listed for this study result from the integration of geomorphological indices and parameters, including *DEI*, slope angle, curvature and *TPI*. Figure 4 summarizes the parameters and synthesis indices used to build this mapping and their respective classes.

For the integration of the parameters and synthesis indices that make up the hydro-geomorphological conditions, weights were assigned to the classes and maps of each terrain condition according to their erosive potential. The generated mappings were intersected, using the Intersect tool (ArcGis 10.7), with the landslide scars inventory shape, and the results supported the establishment of weights for each class, based on the AHP method.

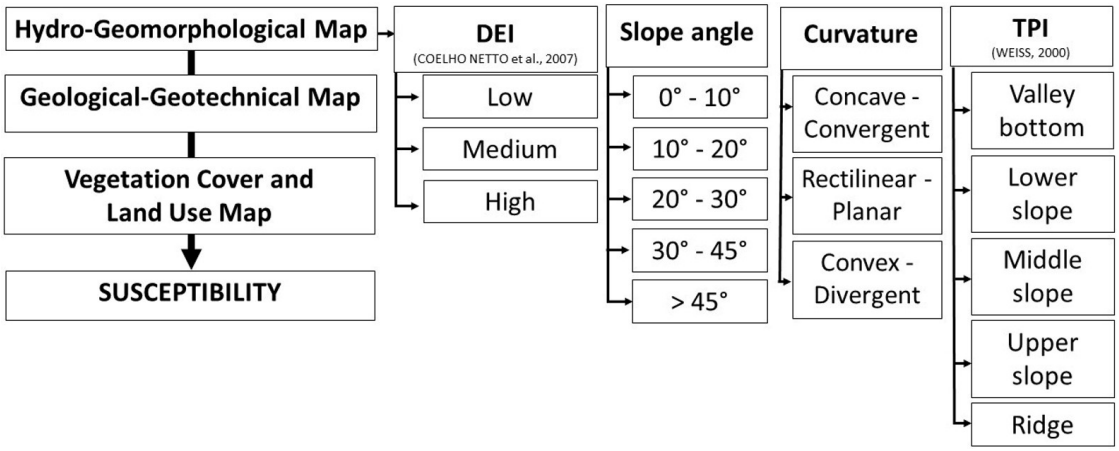

Figure 4. Methodological structure of the geo-hydroecological approach for terrain susceptibility zoning, focusing on the parameters considered relevant for the establishment of Hydro-geomorphological Conditions and the respective classes adopted in this research.

The incidence, which consists of the ratio between the slid area (%) in each class and the area occupied by this class in the basin, was used as a support for establishing weights in the AHP matrix for paired comparison.

The Analytical Hierarchical Process (AHP) was integrated into the geo-hydro-ecological approach to help determine the criteria and weights of each variable used in the crossings. Using the selected criteria, a paired comparison matrix was created to represent the relative importance of classes, based on the attribution of weights and the establishment of priorities. These weights were determined from the Saaty Fundamental Scale, which ranges from 1 to 9, where the value 1 is equivalent to equal importance between the factors and the value 9, the extreme importance of one factor over the other (Saaty, 1994).

In addition to the weight attributed to each class and map, the final weight of the classes (*Pf*) is calculated, which corresponds to the multiplication between the weight of the class (*Pclass*) and the weight of the map (*Pmap*), as shown in Equation 2:

$$Pf = Pclass \times Pmap \quad (2)$$

The shapes corresponding to the *DEI*, slope angle, curvature, and *TPI* were grouped using the *Union* tool (*ArcGis 10.7*). The final weight of the classes was added to obtain the synthesis values, which made it possible to classify the hydro-geomorphological conditions, as suggested by Coutinho (2015). In this sense, the equation applied to obtain the values of hydro-geomorphological conditions was as follows:

$$Pf\ CH = Pf\ Curvature + Pf\ DEI + Pf\ TPI + Pf\ Slope \quad (3)$$

It was decided to work with three classes of erosion potential: Low, Medium, and High, as proposed by Coelho Netto et al. (2007, 2014). The grouping of classes was initially conceived based on the "*Natural breaks*". However, when necessary, adjustments were made according to the characteristics of the terrain.

After the class definition step, the area of the polygons generated from the combination of shapes was calculated. All polygons smaller than 200 m² were merged with neighboring polygons with a larger area or a longer shared border, using the Eliminate tool. This minimum area value was assumed after tests had been carried out with all polygons and with the elimination of polygons with areas < 100 m², < 150 m², < 200 m², < 300 m², and < 400 m² (Figure 5).

The shape including all the generated polygons, in addition to containing many features (> 287,000), presented polygons with very small areas and not representative for the analysis, such as the approximately 44,000 features with an area of less than 1m². The elimination of polygons with areas < 100 m² and < 150 m² showed similar behavior about the distribution of classes, but still with the presence of unrepresentative polygons for mapping.

The elimination of polygons with an area < 200 m² presented a more stimulating result, considering the reduction in the number of features (maintenance of approximately 20% of the initial number of polygons) and the maintenance of the proportion of areas occupied by each class in the basin when compared to the previous tests. The tests carried out with the elimination of polygons < 300 m² and < 400 m² showed a more significant change in the areas occupied by each class, based on the overestimation of the high erosion potential class, to the detriment of the others.

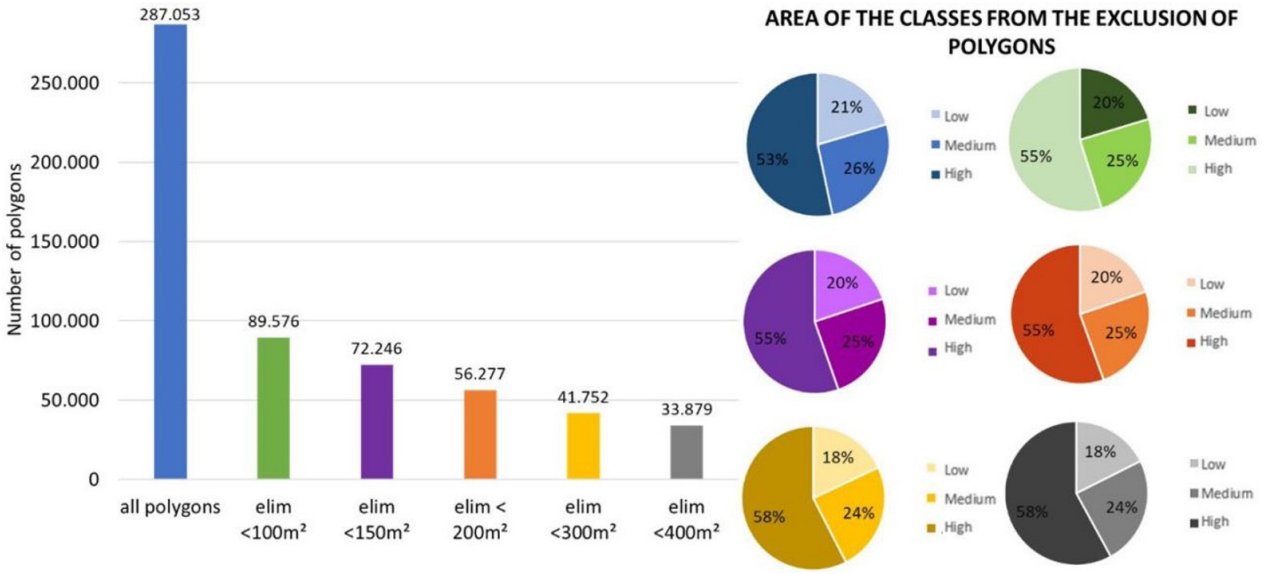

Figure 5. Number of polygons contained in each shape and the area occupied by each class of hydro-geomorphological conditions, from the elimination of polygons depending on the area or maintenance of all polygons generated with the union of the shapes.

Polygons < 200 m² were also eliminated from the curvature, slope angle and *TPI* shapes. It should be noted that, for each area of study and scale of analysis, these values must be revised. Tests need to be carried out so that the elimination of polygons does not lead to an inconsistent reading of the generated files.

3. Analysis and results

3.1 Drainage Efficiency Index (*DEI*)

The results were distributed into three class intervals: low (20.98%), medium (22.65%), and high (56.36%), as shown in Table 1. The low *DEI* class recorded the lowest incidence of landslides (0.40), with a landslide area of 8.37%. The medium *DEI* class concentrated 13% of the slid area and had an incidence of 0.57. The highest percentage of landslides (78.62%) occurred in the high *DEI* class (Table 1; Figure 6), as well as the highest incidence of landslides: 1.39. This class is usually associated with basins with a high topographic gradient and high density of drainage axes and/or concave up topographic hollows.

In the extreme rainfall event of January 2011, the detonation of translational landslides fed other debris flows at the bottom of slope valleys and along the trajectory of river channels. These articulated mass movements constitute a type of complex movement, integrating the processes acting on the slopes with the network of channels that drain the basins at their different hierarchical levels.

In the mountain massif of Tijuca (RJ, Brazil), as well as on the steep slopes of Serra do Mar, in the municipality of Angra dos Reis (RJ, Brazil), Coelho Netto et al. (2007, 2014, respectively) observed that areas with high susceptibility to landslides are associated with the high *DEI* class, in interaction with other geomorphological indices synthesized in the hydro-geomorphological map.

The incidence was used as a support for establishing weights in the AHP matrix for paired comparison (Table 2). An association was sought between the weight of classes and the concentration of landslide area per class (%). For this reason, the high *DEI* class (0.76) assumed the greatest weight, followed by the medium (0.16) and low (0.08) classes. Figure 6 shows the spatialization of the *DEI* in the D'Antas Creek basin.

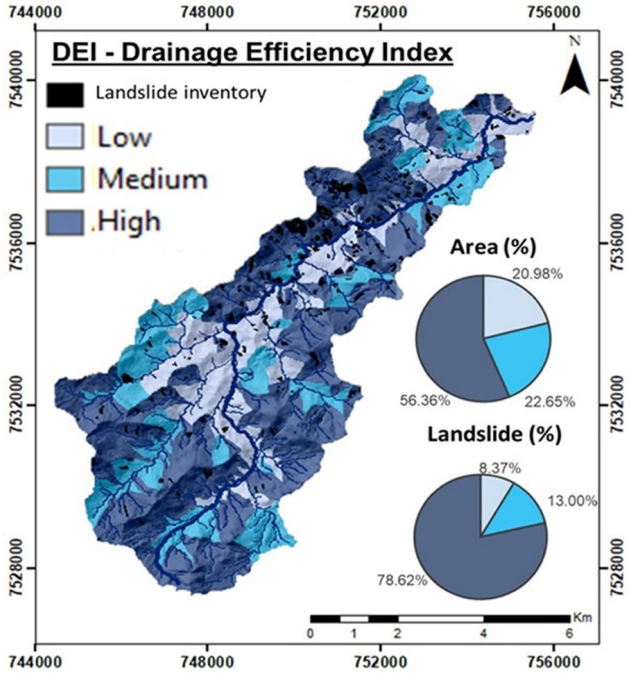

Figure 6. Drainage efficiency index map indicating the area (%) that each class occupies in the basin (adapted from Coutinho, 2015) and the landslide area (%) per class from the inventory of landslides that occurred during the extreme rainfall event in January 2011.

Table 1. Total area in the basin and slid area of each class used in the construction of the Drainage Efficiency Index (*DEI*).

Classes	Class area		Landslide area		Incidence
	km²	%	km²	%	
Low	11.16	20.98	0.08	8.37	0.40
Medium	12.05	22.65	0.12	13.00	0.57
High	29.98	56.36	0.75	78.62	1.39
Total	53.19	100	0.96	100	-

Table 2. AHP matrix of paired comparison between Drainage Efficiency Index (*DEI*) classes.

Classes	High	Medium	Low	Weight
High	1	5	9	0.76
Medium	1/5	1	2	0.16
Low	1/9	1/2	1	0.08

Consistency ratio = 0.001 (< 0.10 consistent).

3.2 Slope angle

The results were distributed into five slope angle classes: 0°–10° (11%); 10°–20° (24.06%); 20°–30° (33.34%); 30°–45º (27.74%); > 45° (3.85%). Crossing the slope angle classes with the landslide inventory showed that 73.04% (279) of the landslide scars had a mean value of slope angle between 30° and 45° (Table 3; Figure 7). The second group with the highest concentration of landslide scars was between 20° and 30° (21.47%; *n* = 82). The classes from 0° to 10°, from 10° to 20° and > 45° were less expressive in the analysis of the mean slopes; when added together, they represented less than 6% (21) of the total number of scars.

How the mean slope of the scars was read enabled a more precise definition of the critical angle in the basin. Although it is difficult to establish precise limits for the critical slope of so-called unstable slopes, values above 30º proved to be highly susceptible to the occurrence of shallow translational landslides in the D'Antas Creek basin. D'Amato Avanzi et al. (2004) in work carried out in the Cardoso basin in northwest Tuscany (Italy) indicate that 84.5% (547) of the assessed landslides occurred on slopes with slope angles between 31° and 45°, among which 35.6% had a gradient of inclination from 36° to 40°. Coelho Netto et al. (2007, 2014), based on Lacerda (1997, 2007) who indicate the critical friction angle for slopes in southeastern Brazil to be around 38°, assume as a critical angle slope angle values greater than 35°.

Cevasco et al. (2013) reported that shallow translational landslides triggered by episodes of intense rain in mountainous areas occur predominantly on slopes with slope angles between 30° and 45°. Steeper slopes generally have little material available for mobilization. Similar results were obtained by Fernandes et al. (2004), based on the analysis of the extreme rainfall event that occurred in the city of Rio de Janeiro in 1996, on the slopes of the Massif of Tijuca (RJ), observed a concentration of shallow landslides in the class between 30º and 55º. In the basins studied by the authors (Quitite and Papagaio), steeper slopes were associated with shallow soils, which could have been slipped previously, suggesting the existence of a threshold angle of inclination for the triggering of landslides.

In the analysis of the landslide area per class, the results assumed the same pattern found with the number of scars. The highest incidence of the slipped area occurred in the class from 30° to 45° (1.99), followed by classes 20° to 30° (1.01), > 45° (0.78), 10°–20° (0 .32), 0°–10° (0.01) as seen in Table 3. Coutinho (2015), when correlating the inventory of landslide scars (*n* = 244) with the slope angle classes (0°–10°; 10°–20°; 20°–35°; > 35°), obtained a concentration of 52.33% of the slid area in the 20°–35° class. However, how the slope angle values were obtained (through polygons representing a class interval) is not representative of the mean value of the landslide scar.

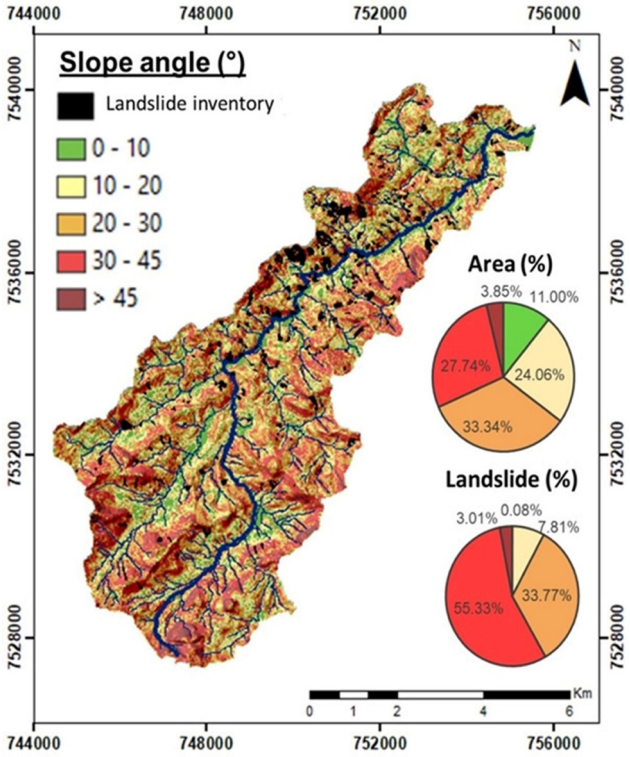

Figure 7. Slope angle map indicating the area (%) that each class occupies in the basin and the landslide area (%) per class from the inventory of landslides that occurred during the extreme rainfall event in January 2011.

Table 3. Total area in the basin and slid area of each class used in the slope analysis.

Classes (°)	Class area		Landslide area		Incidence	Distribution of landslide scars	
	km²	%	km²	%		no.	%
0–10	5.85	11.00	0.00	0.08	0.01	4	1.05
10–20	12.80	24.06	0.07	7.81	0.32	8	2.09
20–30	17.73	33.34	0.32	33.77	1.01	82	21.47
30–45	14.76	27.74	0.53	55.33	1.99	279	73.04
> 45	2.05	3.85	0.03	3.01	0.78	9	2.36
Total	53.19	100	0.96	100	-	382	100

The results obtained for the D'Antas Creek basin are in line with those reported for mountainous domains: extreme rainfall induced landslides tend to occur mainly on slopes angles between 30° and 45°. For this reason, in the AHP paired comparison matrix, the 30°–45° class (0.54) received the highest weight, followed by the 20°–30° class (0.21), as can be seen in Table 4. These two classes together concentrated approximately 90% (0.85 km^2) of the landslide area and 361 (94.50%) landslide scars. Figure 7 presents the slope angle map with the spatial distribution of the classes in the basin and the indication of the percentage of area occupied by each class and landslide area.

3.3 Curvature

The results obtained in an automated mode allowed the definition of three classes: concave-convergent (64.13%), convex-divergent (19.19%), and rectilinear-planar (16.68%). The highest concentration and incidence of landslide areas occurred in the concave-convergent class (75.59%; 1.18), followed by the rectilinear-planar classes (13.42%; 0.80) and convex-divergent (10.81%; 0.56), as observed in Table 5. The visual interpretation of the image also indicates the concave-convergent class as the one with the highest concentration of scars, around 66% (n = 252), followed by the rectilinear-planar class with 22.25% (n = 85) of scars, and the convex-divergent class (11.78%; n = 45).

This result was considered consistent, given the difference in the scale used in each assessment. While the visual interpretation was performed with the aid of contour lines at a scale of 1:5,000, the automated data generation process was based on the pixel value, which represents the smallest unit of measurement in the image. However, both results indicate a strong correlation between this slope geometry and the spatial concentration of shallow landslides. Figure 8 presents the curvature map and the indication of the percentage of occupied area and landslide area in each class.

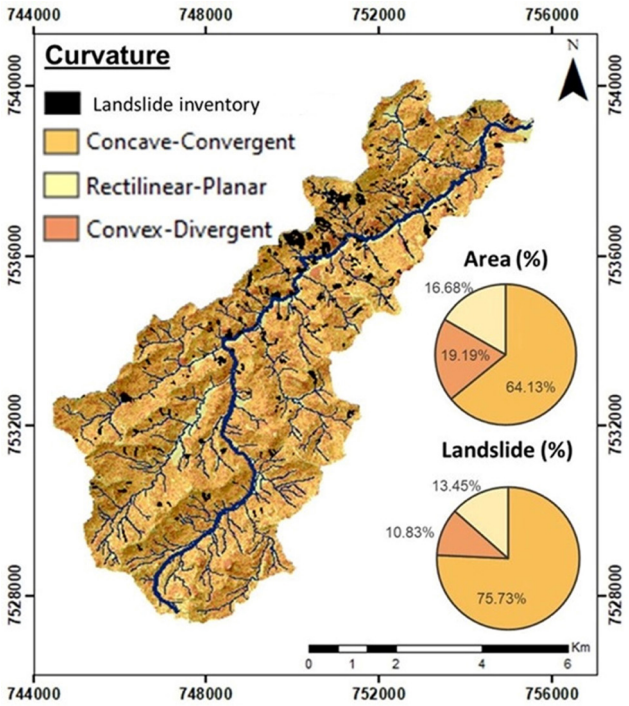

Figure 8. Curvature map indicating the area (%) that each class occupies in the basin and the landslide area (%) per class from the inventory of landslides that occurred during the extreme rainfall event in January 2011.

Table 4. AHP matrix of paired comparison between slope angle classes.

Classes (°)	30–45	20–30	>45	10–20	0–10	Weight
30–45	1	4	7	5	9	0.54
20–30	1/4	1	3	2	7	0.21
>45	1/7	1/3	1	2	3	0.11
10–20	1/5	1/2	1/2	1	3	0.09
0–10	1/9	1/7	1/4	1/5	1	0.04

Consistency ratio = 0.090 (< 0.10 consistent).

Table 5. Area of slope curvature classes, in addition to the slipped area accounted for by the automated mode and number of scars based on visual interpretation.

Classes	Automated Mode					Visual Interpretation (image May/2011)	
	Class area		Landslide area		Incidence	Number of landslide scars	%
	km^2	%	km^2	%			
Concave-Convergent	34.11	64.13	0.73	75.73	1.18	252	65.97
Convex-Divergent	10.21	19.19	0.10	10.83	0.56	45	11.78
Rectilinear-planar	8.87	16.68	0.13	13.45	0.80	85	22.25
Total	53.19	100	0.96	100	-	382	100

The role played by the concave relief compartments in the convergence of surface and subsurface flows has been attested since the studies by Hack & Goodlett (1960), Anderson & Burt (1978), Coelho Netto (1985), Dietrich & Dunne (1993), among others. Hack & Goodlett (1960) defined the concavity axes as the wettest part of the slope system, being able to present channeled flow, especially during rainy periods. This convergence of flows contributes to the development of saturation conditions in soils (Anderson & Burt, 1978). Nseka et al. (2019), in studies in the Kigezi region (southwest Uganda), point out that flow convergence zones (concave shapes), associated with moderately steep slope angles, medium/low slope, high humidity index and flow power index interact and induce the occurrence of landslides.

Research carried out in the southeastern region of Brazil also state that the concave slopes have a dynamic associated not only with the occurrence but also with the recurrence of landslide on the high slopes and accumulation of materials towards the axis of the concavities (Fernandes et al., 2001; Coelho Netto et al., 2016). Coelho Netto et al. (2016) showed this recurrence pattern in a colluvial cone located at the base of a rocky step (height = 10m), in the axis of a concave and steep slope (32º); through a thick sequence of colluviums rich in organic matter (3.5 meters), with radiocarbon ages ranging from 8,990 ± 100 years BP (10,374 to 9,779 cal years BP) at the base to 3,860 ± 100 (4,321 to 3,837 cal years BP) in a layer close to the surface. Studies in the Massif of Tijuca (Rio de Janeiro, RJ) by Fernandes et al. (2004) indicate that the concave shape of the slope presents a potential for failure about three times greater than that obtained in the convex and rectilinear features.

The concave-convergent areas were classified in the paired comparison matrix as being highly susceptible to shallow landslide detonation (0.75). The rectilinear-planar areas assumed a weight of 0.18 since they are the shapes that precede the concavities; therefore, they are subject to the occurrence of shallow landslides (Table 6). The convex-divergent areas, in their turn, were given the lowest weight (0.07) as they disperse water flows, favoring lower pore pressures and terrain stability.

The complexity associated with establishing thresholds adjusted to the study area may explain the low weights attributed to curvature in landslide susceptibility models. Catani et al. (2005), in their landslide susceptibility model (Arno River basin, Italy), state that the curvature, together with lithology and slope gradient, influences the volume and velocity of landslides. However, in the five evaluated areas, the authors point out that the land use (47.3%–10.9%) and the slope gradient (39.6%–14.6%) configure the highest degrees of susceptibility, followed by lithology (23.7%–8.4%), contribution area (30%–1.9%) and curvature (14.4%–2.8%).

Kayastha et al. (2013), evaluating the Tinau watershed (western Nepal), also attributed less weight to the curvature (0.0496) of the slope than to other geomorphological parameters, such as slope angle (0.1703) and aspect (0.0965). The work by Meirelles et al. (2018), developed in the Paquequer River basin (Teresópolis-RJ), points to the shape of the curvature (13.8%) as the third variable in importance to trigger landslides, preceded by slope angle (22.7%) and land use (16.3%). In their turn, Catani et al. (2013) highlight the importance of curvature, as the only variable that is not discarded in the scales evaluated for defining susceptibility models.

The inclusion of the curvature variable in the construction of the hydro-geomorphological conditions map proved to be relevant. The relationship between the forms and processes that gave rise to them constitutes an important precept in understanding the geomorphological evolution of the landscape (Gilbert,1877). Any alteration in the process will be reflected in the forms of the landscape through the readjustment of the parameters, categories, or synthesis indices in search of a new balance. Changes in the forms also influence the regulation of processes and the way they occur.

3.4 Topography Position Index (*TPI*)

The results were distributed into five *TPI* classes: ridge (12.07%), upper slope (13.18%); middle slope (48.45%), lower slope (21.05%), and valley bottom (5.24%). The middle slope class concentrated most of the landslide area, about 57% (0.55 km^2) of the total, representing an incidence of 1.18 of the landslide scars; followed by the upper slope (1.04), lower slope (0.87), ridge (0.76) and valley bottom (0.29), as shown in Table 7. In Figure 9, it is possible to observe the spatialization of the *TPI* classes in the basin, in addition to the landslide area.

Coutinho (2015) also attributed a higher concentration of landslides to the middle slope (49.58%) for the D'Antas Creek basin. Studies conducted by Coelho Netto et al. (2014), in the central area of Angra dos Reis, also indicate that areas with middle slopes, associated with slope angles greater than 35°, are the most susceptible to landslides. Nseka et al. (2019) also point out that in southeastern Uganda landslides are also concentrated (58%) on the middle slope.

Table 6. AHP matrix of paired comparison between the standard curvature classes.

Classes	Concave-convergent	Rectilinear-planar	Convex-divergent	Weight
Concave-convergent	1	3	7	0.75
Rectilinear-planar	1/3	1	3	0.18
Convex-divergent	1/7	1/3	1	0.07

Consistency ratio = 0.03 (< 0.10 consistent).

Although the landslides inventory used for crossing with the terrain conditioning parameters focused on the erosive domain of the scar and did not consider the depositional part (< 10°), there was a concentration of landslides in the lower slope class. Regarding this point, Coelho Netto et al. (2012) call attention to the variation of the geomorphological aspects involved in the rainfall events of 1996 and 2010, which occurred in the city of Rio de Janeiro. While in 1996 the landslides were concentrated from the ridge zone and intermediate interfluves to the valley bottoms, in the 2010 event, detonation prevailed on middle and lower slopes (approximately 60%) (Coelho Netto et al., 2012).

The authors showed that the detonation of landslides can occur in topographically different positions depending on the characteristics of the rainfall event. While in 1996 landslides were associated with steep and elongated slopes, which favored the propagation of mobilized materials and convergence towards valley bottoms, feeding debris flows; in the 2010 event, the high number of occasional landslides (45%) associated with the roads stands out, whether due to high and steep cuts or drainage outlets close to the road's curvatures (Coelho Netto et al., 2012).

These results guided the attribution of weights to the topography position classes (Table 8). The middle slope assumed greater importance (0.54), followed by the upper slope (0.24) and lower slope (0.13) classes. Ridge (0.06) and valley bottom (0.03) had the lowest weights in the paired comparison matrix, due to their little influence on the triggering of shallow landslides.

3.5 Hydro-Geomorphological Map

A synthesis analysis was carried out, attributing the *DEI* (0.38) the greatest importance among the hydro-geomorphological conditions (Table 9). It is an index that synthesizes a set of parameters from a functional reading of the landscape concerning the concentration and direction of flows and humidity on the slopes, which influence the potential for detonation of landslides.

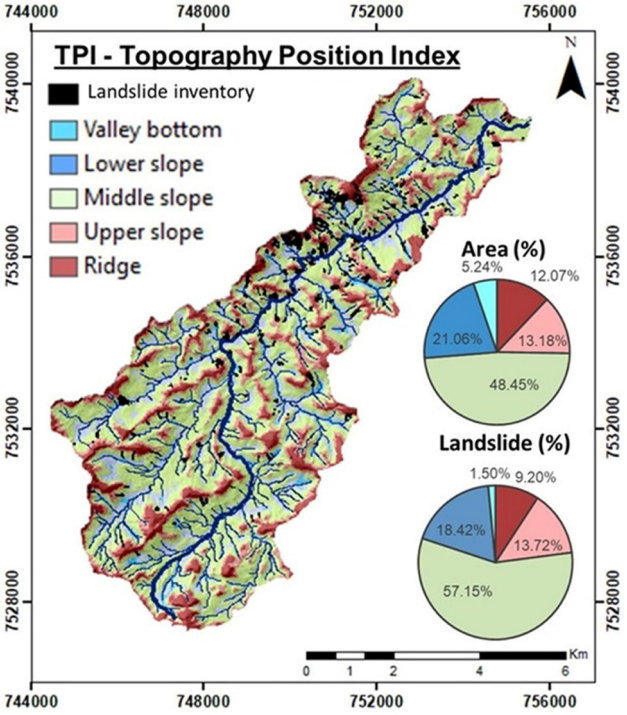

Figure 9. Topography position index map indicating the area (%) that each class occupies in the basin (adapted from Coutinho, 2015) and the landslide area (%) per class from the inventory of landslides that occurred during the extreme rainfall event in January 2011.

Table 7. Total area in the basin and slid area of each class used in the construction of the Topography Position Index (*TPI*).

Classes	Class area		Landslide area		Incidence
	km²	%	km²	%	
Ridge	6.42	12.07	0.09	9.20	0.76
Upper slope	7.01	13.18	0.13	13.72	1.04
Middle slope	25.77	48.45	0.55	57.15	1.18
Lower slope	11.20	21.05	0.18	18.42	0.87
Valley Bottom	2.79	5.24	0.01	1.50	0.29
Total	53.19	100	0.96	100	-

Table 8. AHP matrix of paired comparison between Topography Position Index classes.

Classes	Middle slope	Upper slope	Lower slope	Ridge	Valley Bottom	Weight
Middle slope	1	4	6	8	9	0.54
Upper slope	1/4	1	3	5	7	0.24
Lower slope	1/6	1/3	1	3	5	0.13
Ridge	1/8	1/5	1/3	1	3	0.06
Valley Bottom	1/9	1/7	1/5	1/3	1	0.03

Consistency ratio = 0.071 (< 0.10 consistent).

The slope angle (0.27), which is normally assigned as the main geomorphological parameter in the analysis of terrain susceptibility (Dias et al., 2021a), assumed a similar weight to the curvature (0.22), as both reflect the shape of the slope, based on the gravitational component and the concentration of water flows, respectively (Table 9). The *TPI* was assigned a lower weight (0.13) because it constitutes an approximate measure and delimitation, with a greater degree of generalization of the information.

The terrain conditions adopted and the weights assigned to each of them proved to be adjusted to the conditions of the basin. The data obtained from the inclusion of the curvature in the definition of the erosion potential of the study area were promising, since 88.74% (0.85 km^2) of the landslide area was associated with the class of high erosive potential (Table 10), against 80.05% (0.77 km^2) of landslide area at the intersection between slope angle, *DEI*, and *TPI*, without including slope curvature (Table 11).

The medium class (22.88%) of erosive potential concentrated 7.86% (0.08 km^2) of the landslide area, while the low class (21.03%) erosion potential presented a concentration of 3.40% (0. 03 km^2) of the landslide area. Figure 10 provides an integrated view of the parameters and synthesis indexes that were used to build the hydro-geomorphological conditions map.

The results obtained highlight the importance of using parameters and synthesis indexes of a geomorphological nature in the analysis and classification of the terrain susceptibility. Digital Terrain Models and derived datasets (slope angle, curvature, aspect, surface area, hydrographic pattern, among others) have been highly exploited to obtain geomorphological parameters. However, these parameters need to be inserted in the mappings functionally; that is, allowing one to understand how the processes contribute to the evolution of the landscape and to evaluate how the forms condition the processes at different spatial scales.

It is also important to point out that for each model, the values (or ranges of values) of the input parameters should be adjusted to allow agreement between field observations and automated operations. When adjusted to the conditions of the study area and scale of analysis, the geomorphological parameters are highly promising for the classification of terrain susceptibility to shallow landslides.

Table 9. AHP matrix of paired comparison between hydro-geomorphological conditions.

Classes	*DEI*	Slope angle	Curvature	*TPI*	Weight
DEI	1	2	2	2	0.38
Slope angle	1/2	1	2	2	0.27
Curvature	1/3	1/2	1	2	0.22
TPI	1/5	1/3	1/2	1	0.13

Consistency ratio = 0.081 (< 0.10 consistent).

Table 10. Total area in the basin and landslide area of each class used in the construction of the map of hydro-geomorphological conditions.

DEI, Slope angle, Curvature, *TPI*					
Classes	Class Area		Landslide Area		Incidence
	km^2	%	km^2	%	
Low (0.05795–0.188692)	11.18	21.03	0.03	3.40	0.16
Medium (0.188693–0.376064)	12.17	22.88	0.08	7.86	0.34
High (0.376065–0.662033)	29.84	56.10	0.85	88.74	1.58
Total	53.19	100	0.96	100	-

Table 11. Mapping of hydro-geomorphological conditions without using the curvature parameter.

DEI, Slope angle, *TPI*					
Classes	Class Area		Landslide Area		Incidence
	km^2	%	km^2	%	
Low (0.034660–0.142448)	11.66	21.91	0.04	4.01	0.18
Medium (0.142449–0.263714)	17.9	33.64	0.15	15.94	0.47
High (0.263715–0.513428)	23.64	44.44	0.77	80.05	1.80
Total	11.66	21.91	0.04	4.01	-

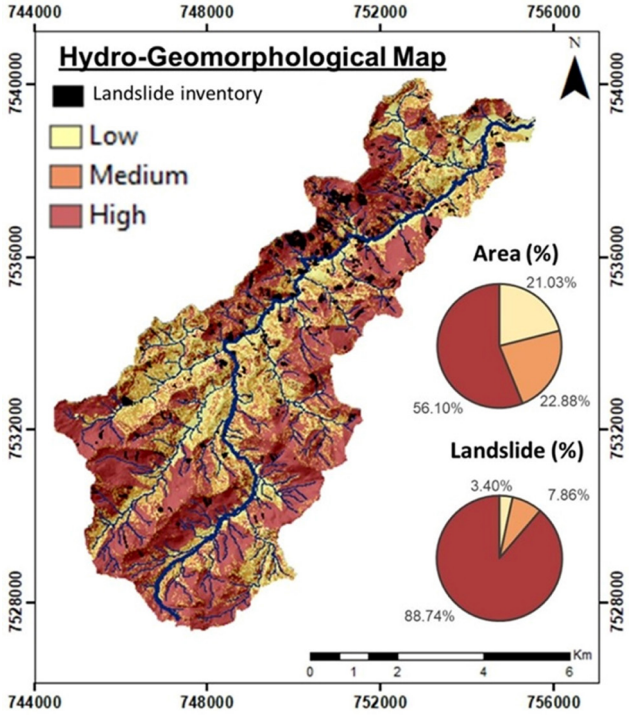

Figure 10. Hydro-geomorphological conditions map indicating the area (%) that each class occupies in the basin and the landslide area (%) per class from the inventory of landslides that occurred during the extreme rainfall event in January 2011.

4. Conclusions

The study of geomorphological parameters has been shown to be highly relevant in integrated analyzes of terrain susceptibility to shallow translational landslides. The functional methodology adopted, integrative of terrain conditions, presents a systemic foundation and organization of the database in a SIG environment. This base remains open for updates, as new functional parameters are identified as relevant, favoring updated diagnoses to guide territorial (re) ordering aimed at preventing, mitigating, and/or adapting human occupation.

How mean slope angle values were obtained for each landslide scar proved to be a significant adjustment for determining the critical slope. The inclusion of the curvature as another condition for the definition of the erosive potential also presented a satisfactory result, with the concentration of more than 87% of the landslide areas in the high erosive potential class. It should be noted that it was not just the inclusion of one more parameter, based on pre-established models, that was conducted. Ranges of values related to curvature were tested in search of a better fit between field observations and automated operations.

The attribution of weights (degree of importance) for each terrain condition was based on a previous analysis that evaluated the behavior of each class of parameters and synthesis indices, considered relevant for the crossing of hydro-geomorphological conditions. The results indicated a significant adjustment between terrain conditions and landslide areas (km^2) and the number of landslide scars. The main objective of this methodological step was to seek ways to bring forecast models closer to the reality of the study area. For this, the AHP method was integrated into the geo-hydro-ecological approach. From a mathematical basis, which allows organizing and examining the relative importance of the criteria, the AHP helped to reduce the inconsistencies of the model.

It is important to point out that the analysis and classification of terrain susceptibility is a continuous process that should be open to updates at time intervals compatible with the pace and variability of landscape transformations. Data concerning the frequency and spatial distribution of landslide should also be permanently open to revision and expansion. The occurrence of new landslides or the reactivation of old ones can provide important information on the rupture mechanisms and/or on the relationship between the occurrence of the movement and the terrain conditions.

Therefore, it is essential that the methodological bases for building and validating these models are available and that they are improved as knowledge advances. Understanding which mapping should be used in each territory, by the public administration, is essential to ensure coherent territorial management in the face of the needs of the population. The use of the resulting map as a planning and territorial management tool should be associated with knowledge of the potentialities and limitations of the generated product.

The questions in this research were stimulated not only by the relevance of landslides in the pattern of evolution of mountainous domains but mainly by the high applied value of this knowledge, since these areas are occupied by cities with a high population contingent, in addition to their socio-environmental, economic and cultural valuations. In this way, the aim is to contribute to a better equation of the risk of disasters.

Acknowledgements

The authors are grateful for the invitation of the scientific committee of VIII COBRAE for the publication of this article. The authors are also grafeful to INCT-REAGEO, the National Council for Scientific and Technological Development (CNPq) and the Carlos Chagas Filho Foundation for Research Support in the State of Rio de Janeiro (FAPERJ), which made this study financially viable.

Declaration of interest

The authors have no conflicts of interest to declare. All co-authors have observed and affirmed the contents of the paper and there is no financial interest to report.

Authors' contributions

Roberta Pereira da Silva: conceptualization, methodology, formal analysis, writing – original draft. Ana Luiza Coelho Netto: conceptualization, methodology, formal analysis, supervision, writing – review & editing. Willy Alvarenga Lacerda: conceptualization, methodology, formal analysis, supervision, writing – review & editing.

Data availability

The data generated and used for the analyzes presented throughout this article are available for scientific use upon request to the authors.

References

Abedini, M., & Tulabi, S. (2018). Assessing LNRF, FR, and AHP models in landslide susceptibility mapping index: a comparative study of Nojian watershed in Lorestan province, Iran. *Environmental Earth Sciences*, *77*, 1-13. http://dx.doi.org/10.1007/s12665-018-7524-1.

Akgun, A., Dag, S., & Bulut, F. (2008). Landslide susceptibility mapping for a landslide-prone area (Findikli, NE of Turkey) by likelihood frequency ratio and weighted linear combination models. *Environmental Geology*, *54*, 1127-1143. http://dx.doi.org/10.1007/s00254-007-0882-8.

Anderson, M.G., & Burt, T.D. (1978). The role of topography in controlling throughflow generation: a reply. *Earth Surface Processes and Landforms*, *3*(4), 331-344. http://dx.doi.org/10.1002/esp.3290030402.

Avelar, A.S., Vinagre, R. & Lacerda, W.A. (2016). Influências Geológicas, Geomorfológicas e Geotecnicas Geotécnicas nos Movimentos de Massa ocorridos nos dias 11 e 12 de janeiro de 2011, em Nova Friburgo, Rio de Janeiro, Brasil. In: *15° Congresso Nacional de Geotecnia e 8° Congresso Luso-Brasileiro de Geotecnia*, Porto, Portugal, 12 p.

Borgomeo, E., Hebditch, K.V., Whittaker, A.C., & Lonergan, L. (2014). Characterising the spatial distribution, frequency and geomorphic controls on landslide occurrence, Molise, Italy. *Geomorphology*, *226*(1), 148-161. http://dx.doi.org/10.1016/j.geomorph.2014.08.004.

Bortoloti, F.D., Castro Junior, R.M., Araújo, L.C., & Morais, M.G.B. (2015). Preliminary landslide susceptibility zonation using GIS-based fuzzy logic in Vitória, Brazil. *Environmental Earth Sciences*, *74*, 2125-2141. http://dx.doi.org/10.1007/s12665-015-4200-6.

Casagli, N., Catani, F., Puglisi, C., Delmonaco, G., Ermini, L., & Margottini, C. (2004). An inventory-based approach to landslide susceptibility assessment and its application to the Virginio River Basin, Italy. *Environmental & Engineering Geoscience*, *10*(4), 203-216. http://dx.doi.org/10.2113/10.3.203.

Catani, F., Casagli, N., Ermini, L., Righini, G., & Menduni, G. (2005). Landslide hazard and risk mapping at catchment scale in the Arno River basin. *Landslides*, *2*, 329-342. http://dx.doi.org/10.1007%2Fs10346-005-0021-0.

Catani, F., Lagomarsino, D., Segoni, S., & Tofani, V. (2013). Landslide susceptibility estimation by random forests technique: sensitivity and scaling issues. *Natural Hazards and Earth System Sciences*, *13*(11), 2815-2831. http://dx.doi.org/10.5194/nhess-13-2815-2013.

Cevasco, A., Pepe, G., & Brandolini, P. (2013). The influences of geological and land use settings on shallow landslides triggered by an intense rainfall event in a coastal terraced environment. *Bulletin of Engineering Geology and the Environment*, *73*(3), 859-875. http://dx.doi.org/10.1007/s10064-013-0544-x.

Coelho Netto, A.L. (1985). *Surface hydrology and soil erosion in a tropical mountainous rainforest drainage basin, Rio de Janeiro* [Doctoral thesis]. Katholieke University Leuven.

Coelho Netto, A.L., Avelar, A.S., Fernandes, M.C., & Lacerda, W.A. (2007). Landslide susceptibility in a mountainous geoecosystem, Tijuca Massif, Rio de Janeiro: the role of morphometric subdivision of the terrain. *Geomorphology*, *87*(3), 120-131. http://dx.doi.org/10.1016/j.geomorph.2006.03.0.

Coelho Netto, A.L., Avelar, A.S., Fernandes, M.C., Coutinho, B., & Freitas, L. (2008). *Relatório Técnico da Qualidade Ambiental do Estado do Rio de Janeiro (1:100.000): subsídios para o zoneamento econômico-ecológico*. Secretaria de Meio Ambiente do Governo do Estado do Rio de Janeiro.

Coelho Netto, A.L., Avelar, A.S., Sato, A.M., Dias, M.A., & Negreiros, A.B. (2012). Vulnerabilidade em geoecossistemas montanhosos e desastres causados por deslizamentos na interface florestal-urbana: controles geológicos, geomorfológicos e geoecológicos. In W.L. Lacerda, E.M. Palmeiras, A.L. Coelho Netto & M. Ehrlich (Eds.), *Desastres naturais: susceptibilidade e riscos, mitigação e prevenção, gestão e ações emergenciais*. COPPE/UFRJ.

Coelho Netto, A.L., Avelar, A.S., Sato, A.M., Fernandes, M.C., Oliveira, R.R., Vinagre, R., Barbosa, L., Lima, P.H., & Lacerda, W.L. (2014). Landslide susceptibility and risk zoning at Angra dos Reis, Rio de Janeiro state, southeast Brazil: a quali-quantitative approach at 1:5000 scale. In In W.L. Lacerda, E.M. Palmeiras, A.L. Coelho Netto & M. Ehrlich (Eds.), *Extreme rainfall induced landslides: an international perspective* (pp. 262-296). Oficina de Textos.

Coelho Netto, A.L., Facadio, A.C., & Silva, R.P. (2020). Geomorfologia do Estado do Rio de Janeiro e zona de fronteira: uma abordagem geo-hidroecológica. In M.E. Dantas, J.M. Morais, M.A. Ferrassoli, M.Q. Jorge & V. A. Hilquias (Eds.), *Geodiversidade do Estado do Rio de Janeiro - Programa Geologia do Brasil - Levantamentos da Geodiversidade* (1. ed., Vol. 1, pp. 125-186). Serviço Geológico do Brasil - CPRM.

Coelho Netto, A.L., Sato, A., Avelar, A.S., Vianna, L.G., Araújo, I., Ferreira, D., Lima, P., Silva, A., & Silva, R.P. (2013). January 2011: The Extreme Landslide Disaster in Brazil. In C. Margottini, P. Canuti & K. Sassa (Eds.), *Landslide science and practice* (pp. 377-384). Springer-Verlag Berlin Heidelberg.

Coelho Netto, A.L., Silva, R.P., Facadio, A.C., & Lima, P.H. (2016). Movimentos gravitacionais de massa e evolução das encostas montanhosas em regiões tropicais: estudos em Nova Friburgo, RJ. In A.L.L.S. Nunes, C.F. Mahler, F.A.B. Danziger, F.J.C.O. Castro, F.R. Lopes, F.T.S. Aragão, I.S.M. Martins, L.M.G. Motta, M.S.S. Almeida, M.C. Barbosa, M. Ehrlich (Eds.), *Willy Lacerda: doutor no saber e na arte de viver* (pp. 235-241). Outras Letras.

COPPETEC/SEA-RJ. (2010). *Mapeamento (Escala 1:5 000) de áreas de riscos, frente aos escorregamentos de encostas no município de Angra Dos Reis, RJ*. Fundação Coordenação de Projetos, Pesquisas e Estudos Tecnológicos/Secretaria de Estado do Meio Ambiente – Governo do Estado do Rio de Janeiro.

COPPETEC/SMAC-RJ. (2000). *Diagnóstico/Prognóstico sobre a Qualidade Ambiental do Geoecossistema do Maciço da Tijuca - subsídios à regulamentação da APARU do Alto da Boa Vista*. Fundação Coordenação de Projetos, Pesquisas e Estudos Tecnológicos/Secretaria de Estado do Meio Ambiente - Prefeitura da Cidade do Rio de Janeiro.

Coutinho, B.H. (2015). *Indicadores geo-hidroecológicos de suscetibilidade das encostas frente a erosão e movimentos de massa em região montanhosa tropical úmida: suporte metodológico para zoneamentos de riscos em diferentes escalas de análise espacial* [Doctoral thesis]. Universidade Federal do Rio de Janeiro. (in Portuguese)

D'Amato Avanzi, G., Giannecchini, R., & Puccinelli, A. (2004). The influence of the geological and geomorphological settings on shallow landslides, An example in a temperate climate environment:the June 19, 1996 event in north-western Tuscany (Italy). *Engineering Geology*, *73*(3-4), 215-228. http://dx.doi.org/10.1016/j.enggeo.2004.01.005.

Dias, H., Hölbling, D., & Grohmann, C. (2021a). Landslide Susceptibility Mapping in Brazil: a review. *Geosciences*, *11*(10), 1-15. http://dx.doi.org/10.3390/geosciences11100425.

Dias, H.C., Gramani, M.F., Grohmann, C.H., Bateira, C., & Vieira, B.C. (2021b). Statistical-based shallow landslide susceptibility assessment for a tropical environment: a case study in the southeastern Brazilian coast. *Natural Hazards*, *108*, 205-223. http://dx.doi.org/10.1007/s11069-021-04676-y.

Dietrich, W.E., & Dunne, T. (1993). The channel head. In K. Beven & M.J. Kirkby (Eds.), *Channel network hydrology* (pp. 175-219). John Wiley & Sons.

ESRI. (2019). *Curvature function*. ArcGis. Retrieved in October 10, 2022, from https://desktop.arcgis.com/en/arcmap/10.7/manage-data/raster-and-images/curvature-function.htm.

Fell, R., Corominas, J., Bonnard, C., Cascini, L., Leroi, E., & Savage, W.Z. (2008). Guidelines for landslide susceptibility, hazard and risk zoning for land use planning. *Engineering Geology*, *102*(3-4), 85-98. http://dx.doi.org/10.1016/j.enggeo.2008.03.022.

Fernandes, N.F., Guimarães, R.F., Gomes, R.T.A., Vieira, B.C., Montgomery, D.R., & Greenberg, H. (2001). Condicionantes geomorfológicos dos deslizamentos nas encostas: avaliação de metodologias e aplicação de modelo de previsão de áreas susceptíveis. *Revista Brasileira de Geomorfologia*, *2*(1), 51-71. [in Portuguese]

Fernandes, N.F., Guimarães, R.F., Gomes, R.T.A., Vieira, B.C., Montgomery, D.R., & Greenberg, H. (2004). Topographic controls of landslides in Rio de Janeiro: field evidence and modeling. *Catena*, *55*(2), 163-181. http://dx.doi.org/10.1016/S0341-8162(03)00115-2.

Gao, J. (1993). Identification of topographic settings conducive to landsliding from dem in Nelson county, Virginia, U.S.A. *Earth Surface Processes and Landforms*, *18*(7), 579-591. http://dx.doi.org/10.1002/esp.3290180702.

Gilbert, G.K. (1877). *Report on the geology of the Henry mountains*. U.S. Department of the Interior. https://doi.org/10.3133/70039916.

Guzzetti, F., Ardizzone, F., Cardinali, M., Galli, M., Reichenbach, P., & Rossi, M. (2008). Distribution of landslides in the Upper Tiber River basin, central Italy. *Geomorphology*, *96*(1-2), 105-122. http://dx.doi.org/10.1016/j.geomorph.2007.07.015.

Hack, J.T., & Goodlett, J.C. (1960). *Geomorphology and forest ecology of a mountain region in the central Appalachians - Professional Paper 347*. U.S. Department of the Interior. https://dx.doi.org/10.3133/pp347.

Jenks, G.F. (1977). *Optimal data classification for choropleth maps*. Lawrence, KS: University of Kansas, Department of Geography, 24 p.

Jenness, J. (2006). *Topograhic Position Index (tpi_jen.avx) extensión for ARCView 3.X, v.1.3a*. Jennes Enterprises. Retrieved October 10, 2022, from http://www.jennessent.com/arcview/tpi.htm.

Kayastha, P., Megh Raj, D., & De Smedt, F. (2013). Application of the Analytical Hierarchy Process (AHP) for landslide susceptibility mapping: a case study from the Tinau watershed, west Nepal. *Computers & Geosciences*, *52*, 398-408. http://dx.doi.org/10.1016/j.cageo.2012.11.003.

Lacerda, W.A. (1997). Stability of natural slopes along the tropical coast of Brazil. In *Proceedings of the Internacional Symposium on Recent Developments in Soil and Pavement Mechanics* (pp. 17-39). Rio de Janeiro. Balkema.

Lacerda, W.A. (2007). Landslide initiation in saprolite and colluvium in southern Brazil: field and laboratory observations. *Geomorphology*, *87*(3), 104-119. http://dx.doi.org/10.1016/j.geomorph.2006.03.03.

Larsen, M.C., & Torres-Sánchez, A.J. (1998). The frequency and distribution of recent landslides in three montane tropical regions of Puerto Rico. *Geomorphology*, *24*(4), 309-331. http://dx.doi.org/10.1016/s0169-555x(98)00023-3.

Martha, T.R., Roy, P., Govindharaj, K.B., Kumar, K.V., Diwakar, P.G., & Dadhwal, V.K. (2014). Landslides triggered by the June 2013 extreme rainfall event in parts of Uttarakhand state, India. *Landslides*, *12*(1), 135-146. http://dx.doi.org/10.1007/s10346-014-0540-7.

Meirelles, E., Dourado, F., & Castilho da Costa, V. (2018). Análise multicritério para mapeamento da suscetibilidade a movimentos de massa na bacia do rio Paquequer-RJ. *Geo UERJ*, *33*, 1-22. https://dx.doi.org/10.12957/geouerj.2018.26037.

Nakileza, B.R., & Nedala, S. (2020). Topographic influence on landslides characteristics and implication for risk management in upper Manafwa catchment, Mt Elgon Uganda. *Geoenvironmental Disasters*, *7*(27), 1-13. http://dx.doi.org/10.1186/s40677-020-00160-0.

Nohani, E., Moharrami, M., Sharafi, S., Khosravi, K., Pradhan, B., Pham, B.T., Lee, S.M., & Melesse, A. (2019). Landslide susceptibility mapping using different gis-based bivariate models. *Water (Basel)*, *11*(1402), 1-22. http://dx.doi.org/10.3390/w11071402.

Nseka, D., Kakembo, V., Bamutaze, Y., & Mugagga, F. (2019). Analysis of topographic parameters underpinning landslide occurrence in Kigezi highlands of southwestern Uganda. *Natural Hazards*, *99*, 973-989. http://dx.doi.org/10.1007/s11069-019-03787-x.

Ribeiro, M.C., Metzger, J.P., Martensen, A.C., Ponzoni, F.J., & Hirota, M.M. (2009). The Brazilian Atlantic Forest: how much is left, and how is the remaining forest distributed? Implications for conservation. *Biological Conservation*, *142*(6), 1141-1153. http://dx.doi.org/10.1016/j.biocon.2009.02.021.

Saaty, T.L. (1994). How to make a decision: the analytic hierarchy process. *Interfaces*, *24*, 19-43. http://dx.doi.org/10.1287/inte.24.6.19.

Seif, A. (2014). Using Topographic Position Index for landform classification (Case study: Grain Mountain). *Bulletin of Environment, Pharmacology and Life Sciences*, *3*, 33-39.

Silva, R.P., Lacerda, W.A., & Coelho Netto, A.L. (2022). Relevant geological-geotechnical parameters to evaluate the terrain susceptibility for shallow landslides: nova Friburgo, Rio de Janeiro, Brazil. *Bulletin of Engineering Geology and the Environment*, *81*, 1-18. http://dx.doi.org/10.1007/s10064-021-02557-z.

Silva, R.P., Lima, P.H.M., Facadio, A.C., & Coelho Netto, A.L. (2016). Condicionantes geomorfológicos e geológicos relacionados à deflagração de movimentos gravitacionais de massa: bacia do Córrego Dantas, Nova Friburgo – RJ. In *Anais do XI Simpósio Nacional de Geomorfologia* (pp. 1-7). Maringá. UGB.

Strahler, A. (1952). Dynamic Basis of Geomorphology. *Geological Society of America Bulletin*, *63*(9), 923-993. http://dx.doi.org/10.1130/0016-7606(1952)63[923:DBOG]2.0.CO;2.

Tagil, S., & Jenness, J. (2008). GIS-Based automated landform classification and topographic, landcover and geologic attributes of landforms around the Yazoren Polje, Turkey. *Journal of Applied Sciences*, *8*(6), 910-921. http://dx.doi.org/10.3923/jas.2008.910.921.

Valeriano, M.D.M. (2008). *Topodata: guia para utilização de dados*. INPE. Retrieved in October 10, 2022, from http://urlib.net/ibi/8JMKD3MGP8W/33EPEBL.

Varnes, D.J. (1978). Slope movement types and processes. In R.L. Schuster & R.J. Krizek (Eds.), *Landslides: analysis and control* (pp. 11-33). National Academy of Sciences. Retrieved in November 12, 2023, from https://onlinepubs.trb.org/Onlinepubs/sr/sr176/176-002.pdf.

Veloso, R.B., Rangel Filho, A.L.R., & Lima, J.C.A. (1991). *Classificação da vegetação brasileira, adaptada a um sistema universal*. IBGE. Retrieved in October 10, 2022, from https://jbb.ibict.br/handle/1/397.

Wang, Q., Li, W., Chen, W., & Bai, H. (2015). GIS-based assessment of landslide susceptibility using certainty factor and index of entropy models for the Qianyang County of Baoji city, China. *Journal of Earth System Science*, *124*, 1399-1415. http://dx.doi.org/10.1007/s12040-015-0624-3.

Weiss, A.D. (2000). *Topographic position and landforms analysis*. Jenness Enterprises. Retrieved in October 10, 2022, from http://www.jennessent.com.